energy&fuels

pubs.acs.org/EF Article

Comprehensive Compositional and Structural Comparison of Coal and Petroleum Asphaltenes Based on Extrography Fractionation Coupled with Fourier Transform Ion Cyclotron Resonance MS and MS/MS Analysis

Sydney F. Niles, Martha L. Chacón-Patiño, Donald F. Smith, Ryan P. Rodgers,* and Alan G. Marshall*

Cite This: *Energy Fuels* 2020, 34, 1492−1505 Read Online

ACCESS | Metrics & More | Article Recommendations | Supporting Information

ABSTRACT: A recently developed extrography separation method fractionates petroleum asphaltenes based on their ionization efficiency, which correlates with polarity, aggregation tendency, and asphaltene structure (single-core or island versus multicore or archipelago). Archipelago asphaltenes were recently demonstrated to coexist with island structures in a variety of petroleum samples; however, archipelago compounds ionize much less efficiently than island compounds, making the former difficult to observe by mass spectrometry without prior separation. Highly processed coal-derived asphaltenes have been studied previously to reveal only small, single-core structure asphaltenes; however, the structure(s) of asphaltenes from unaltered coal extracts has not been extensively studied. Thus, this work focuses on the application of the extrography separation to an unaltered Illinois coal No. 6 asphaltene extract to reveal the coexistence of island and archipelago structural motifs by positive-ion (+) atmospheric pressure photoionization (APPI) Fourier transform ion cyclotron resonance mass spectrometry. Asphaltenes from a Wyoming crude oil sample are also characterized for comparison with coal asphaltenes. The results reveal that Wyoming crude oil asphaltenes contain mainly island species, whereas coal asphaltenes contain archipelago and island compounds with high oxygen content. The structural analysis is enabled by a new "multinotch" stored-waveform inverse Fourier transform isolation, which selectively isolates high-aromaticity precursor ions at each of several nominal mass ranges prior to fragmentation by infrared multiphoton dissociation, and enables unambiguous determination of island versus archipelago species in samples that contain compounds with high and low aromaticity. The more polarizable fractions from each asphaltene sample reveal low-aromaticity polyfunctional oxygenated species, with a solubility behavior consistent with asphaltenes but a compositional range typical of maltenes. These atypical asphaltene species, which ionize poorly, are hypothesized to participate in multiple hydrogen bonding interactions and thus exhibit strong adsorption on polar stationary phases such as SiO_2. Furthermore, these polarizable polyfunctional species ionize preferentially as protonated cations by (+) APPI, accounting for their capability to hydrogen-bond in solution. Collectively, the results demonstrate the existence of archipelago structures in both coal and petroleum asphaltenes, along with polyoxygenated species with low aromaticity that behave like asphaltenes in terms of solubility, because they can establish stronger intermolecular forces such as hydrogen bonding.

INTRODUCTION

Archipelago Asphaltenes in Petroleum. Recent advances in petroleum asphaltene characterization by Fourier transform ion cyclotron resonance mass spectrometry (FT-ICR MS) coupled with an offline, novel separation method based on MS ionization efficiency have demonstrated that petroleum asphaltenes are ultracomplex mixtures of island and archipelago structures.[1−3] Island-type asphaltenes contain a single aromatic core with alkyl side chains, whereas archipelago asphaltenes consist of multiple aromatic cores interconnected by aryl or alkyl linkages. Recent reports demonstrate that both motifs coexist in petroleum asphaltenes and reveal a structural continuum increasingly enriched in archipelago motifs as a function of increasing oxygen content, aggregation tendency, and molecular weight.[2,3] The dominance of one structural motif over the other depends on geological origin, and their quantification ultimately provides an accurate means to maximize valuable products from asphaltene-rich feedstocks.[3] The discovery of archipelago motifs in petroleum has enabled the identification of the most problematic fraction of asphaltenes as they have been shown to disproportionally aggregate and are hypothesized to be the dominant fraction that causes deposition and fouling problems in production and refining.[2−4]

Molecular Structure of Asphaltenes Derived from Upgraded Coal Samples. Previous reports suggest that the heptane-insoluble/toluene-soluble compounds (asphaltene fraction) from coal-derived liquids are smaller in size, with fewer fused aromatic rings than petroleum asphaltenes.[5,6] Others claim that island structures are the sole motif in coal-derived asphaltenes, regardless of their molecular weight, heteroatom content, and/or geological origin.[6−10] Some

Received: October 15, 2019
Revised: December 14, 2019
Published: February 4, 2020

https://dx.doi.org/10.1021/acs.energyfuels.9b03527
Energy Fuels 2020, 34, 1492−1505

studies report that the most abundant species from coal-derived and petroleum asphaltenes contain a similarly sized aromatic core; however, coal-derived asphaltenes generally exhibit shorter alkyl side chains, accounting for the discrepancy between coal and petroleum asphaltene molecular sizes.[8,9] Prior research also suggests that coal-derived asphaltenes are enriched in more cata-condensed structures than peri-condensed cores, compared with petroleum asphaltenes.[5,10] Furthermore, coal-derived asphaltenes have been reported to contain more pyrrole and phenolic functionalities.[5] Hydrogen-bonding interactions as well as $\pi-\pi$ stacking have been implicated as the dominant intermolecular forces between coal asphaltenes.[5] Less alkylation in coal asphaltenes enables strong aggregation by $\pi-\pi$ interactions between the aromatic cores, whereas petroleum asphaltenes, with high alkylation, exhibit stronger steric hindrance and thus less $\pi-\pi$ stacking interaction between the cores. Coal pyrolysis products have been analyzed by negative-ion (−) electrospray ionization (ESI) FT-ICR MS to reveal high abundance of acidic oxygenated species. However, it is important to point out that unmodified coal asphaltenes have not been extensively studied by high-resolution MS and pyrolysis of coal asphaltenes has been demonstrated to break carbon−carbon linkages (possibly between aromatic cores).[11,12] Most reports about the molecular characterization of coal asphaltenes focus on asphaltenes from coal-derived liquids, which have been heavily processed through hydrogenation, catalytic hydrotreating, pyrolysis, and/or liquefaction,[10,11,13−15] which may alter asphaltene structure.[16] Enhanced knowledge of unmodified coal asphaltene structure may allow for better utilization of coal in energy production.[17]

Wu et al. reported the characterization of acidic species in pyridine extracts from Illinois No. 6 coal and Pocahontas No. 3 coal by (−) ESI FT-ICR MS.[18,19] Comparison of these two coal extracts revealed higher levels of O_2 and NO_2 species in both coal samples and showed different degrees of alkylation between coal compounds from different geological origins.[18] The Illinois coal No. 6 extract revealed various different heteroatom classes, with more oxygen- and sulfur-containing species (O_3, NO_3, O_3S) than the Pocahontas No. 3 coal extract, which contained more nitrogen-containing compounds (N, NO, N_2O, NO_3, NS). Acidic *n*-hexane-insoluble species (asphaltenes) from Illinois No. 6 coal were isolated from the pyridine extract and characterized by (-) ESI FT-ICR MS to reveal higher aromaticity and oxygen content than the unfractionated coal extract.[20] However, no structural analysis of asphaltenes was performed, and only acidic species were accessed by (-) ESI.[20] Recently, positive-ion (+) atmospheric pressure photoionization (APPI) has been demonstrated to be a preferred ionization technique for asphaltenes due to its ability to effectively ionize highly aromatic species that are prevalent in asphaltenes.[21−24]

Extrography Separation and Monomer Ion Yield. A recently introduced separation method involves the adsorption of asphaltenes onto silica gel followed by a series of Soxhlet extractions to separate compounds by ionization efficiency.[2] Furthermore, that separation enables both island and archipelago asphaltenes to be observed by mass spectrometry because they are extracted in different fractions. The extrography method has been applied to numerous petroleum samples and has demonstrated the coexistence of island- and archipelago-type compounds in a variety of asphaltenes.[3] Here, we apply the method to petroleum (Wyoming crude oil) and coal (Illinois No. 6 coal) asphaltenes for comparison and structural determination. Wyoming crude oil was chosen because extrography separation has previously been conducted for Wyoming deposit asphaltenes, which are dominated by single-core/island structures.[3] The Illinois coal No. 6 sample has previously been demonstrated to be the most chemically diverse coal sample from the Argonne coal supply and thus is widely used as a coal standard.[18−20,25−28] However, much remains unknown about the asphaltene fraction of unmodified coal extracts and whether they contain archipelago asphaltenes similar to those in petroleum. It is important to point out that the molecular-level characterization of coal is difficult because of its high oxygen content, even for maltenes (*n*-heptane/toluene-soluble). That behavior is contrary to petroleum maltenes, well known to be depleted in heteroatom content relative to petroleum asphaltenes.

The extrography separation extends the characterization of asphaltenic samples through mass spectrometric detection of species not observable for unfractionated samples due to ∼10 to 140-fold differences in ionization efficiencies.[2,29] The extrography method comprises two solvent series. The first is acetone and acetonitrile, which extract compounds that ionize efficiently by (+) APPI for mass spectrometry analysis. Acetone and acetonitrile have also been demonstrated to extract peri-condensed polycyclic aromatic hydrocarbons and porphyrins.[30] The second is an eluotropic series of solvents that extract compounds by polarity. The series includes *n*-heptane, *n*-heptane/toluene (Hep/Tol), toluene, toluene/tetrahydrofuran (Tol/THF), THF, and THF/methanol (MeOH).

The latest/polar fractions typically require longer accumulation period to attain a target signal magnitude optimal for data collection, reflecting a lower ionization efficiency or lower monomer ion yield. Monomer ion yield is calculated as previously described and is inversely proportional to the length of time required to collect a target number of ions for a sample at a given concentration.[1] Therefore, monomer ion yield reflects the ion production efficiency as measured by mass spectrometry. Previous work for petroleum asphaltenes has suggested that the polar fractions contain asphaltenes with stronger aggregation trends in Hep/Tol than their nonpolar counterparts.[2] The polar fractions reveal a higher proportion of archipelago motifs and also exhibit lower monomer ion yields, suggesting a possible correlation between aggregation tendency and ionization efficiency.[2] Because mass spectrometry enables observation only of those compounds which ionize easily, prior separations are critical to observe difficult-to-ionize fractions containing polarizable/archipelago species.

Structural Determination by Multinotch SWIFT Isolation and IRMPD. The present approach focuses on selective fragmentation of high-double-bond-equivalents (DBE = number of rings plus double bonds to carbon) precursor ions for definitive identification of archipelago species. For structural determination of asphaltenes, ions from the high-aromaticity (high DBE, thus, low hydrogen content) portion spanning a small m/z range (4 Da) are isolated prior to fragmentation with a quadrupole mass filter and a new multinotch stored waveform inverse Fourier-transform (SWIFT) waveform method (see Experimental Methods). The removal of low-DBE precursor ions provides definitive assignment of molecular motifs because a high-DBE precursor ion can yield low-DBE fragments only if it is multicore (archipelago). If no low-DBE fragments are observed, the

https://dx.doi.org/10.1021/acs.energyfuels.9b03527
Energy Fuels 2020, 34, 1492−1505

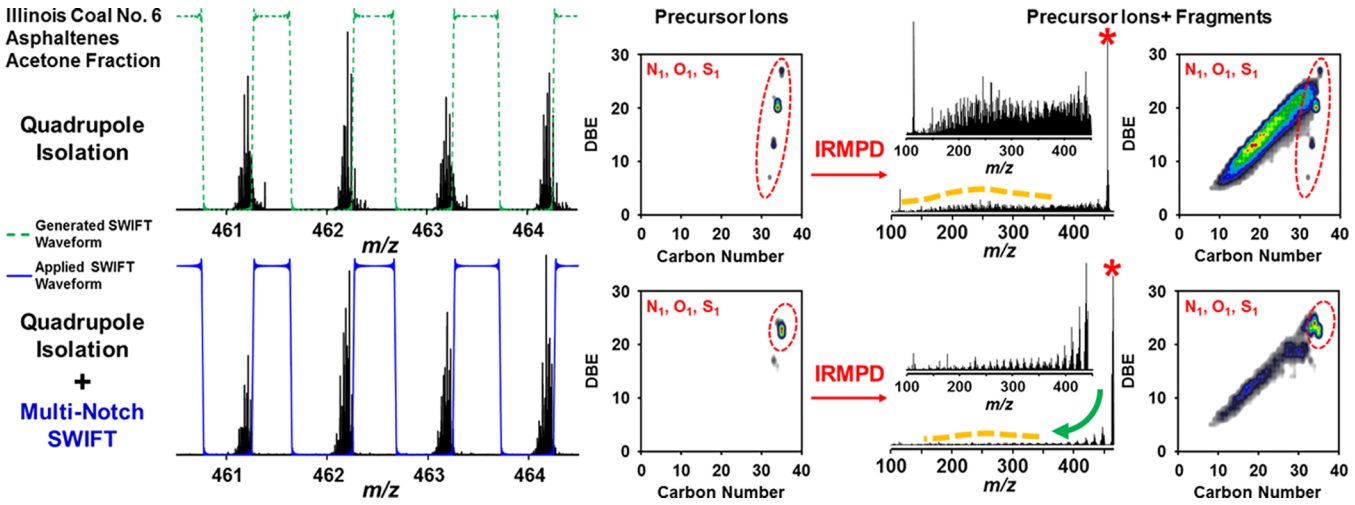

Figure 1. Comparison of quadrupole versus multinotch SWIFT isolations of Illinois Coal No. 6 asphaltenes (acetone fraction) prior to fragmentation by IRMPD. Mass spectra (left) of precursor ions for quadrupole isolation (top) and multinotch SWIFT isolation (bottom) for m/z 461−465, along with isoabundance-contoured plots of (DBE = number of rings plus double bonds to carbon) versus carbon number for N_1, O_1, and S_1 precursor ions (red). Fragmentation product ion mass spectra (right) of precursor and fragment ions from (top) quadrupole isolation and (bottom) multinotch SWIFT isolation for m/z 100−465, along with zoom inset mass spectra of fragment ions without the precursors (m/z 100−450). Corresponding isoabundance-contoured plots of DBE versus carbon number for N_1, O_1, and S_1 precursor ions (red) and fragments are shown (far right, top) for quadrupole isolated and (bottom) SWIFT-isolated compounds.

asphaltene is single-core (island)-dominant. Without removal of low-DBE precursors prior to fragmentation, the presence of low-DBE fragments (after fragmentation) cannot provide definitive proof of multicore structures because they may have been present prior to the fragmentation. Thus, this method enables unambiguous identification of archipelago structures. Infrared multiphoton dissociation (IRMPD) of asphaltene fractions in the ICR cell was employed to reveal structural differences between petroleum/coal samples and fractions. It is important to point out that the dissociation of complex mixtures inside the ICR cell prevents secondary reactions due to ultrahigh vacuum (4.5×10^{-10} Torr), enabling confident analysis of the asphaltene structure. Coal asphaltenes were previously thought to be all island-type; however, the present approach, combining separations, FT-ICR MS, and SWIFT multinotch isolation of high-DBE precursor ions, provides evidence for the co-existence of single-core and multicore structures in petroleum and coal-extract asphaltenes.

EXPERIMENTAL METHODS

Materials. A glass ampule of Illinois coal No. 6 (10 grams, −20 mesh) was acquired from the Argonne Premium Coal Sample Bank. Wyoming crude oil was supplied by Nalco Champion and used for asphaltene isolation for comparison with coal asphaltenes. HPLC-grade tetrahydrofuran (THF) with no solvent stabilizer was obtained from Alfa Aesar (Ward Hill, MA). HPLC-grade *n*-heptane, acetone, toluene, methanol, acetonitrile, and dichloromethane were purchased from JT Baker chemicals (Phillipsburg, PA). All solvents were used as received.

Extraction of Coal Compounds. Soluble coal compounds were extracted with a Soxhlet apparatus equipped with a solvent mixture of 9/9/2 toluene/THF/methanol for 5 days. The extract was dried under N_2 gas, and the extracted coal compounds were subjected to asphaltene precipitation as described below.

Precipitation of Asphaltenes. A previously described method[1] was used for precipitation of C_7 asphaltenes for the Illinois coal extract and Wyoming crude oil. In short, 1 mL of crude oil/coal extract was mixed with 40 mL of *n*-heptane under sonication and refluxed heating at 90 °C. The mixture was allowed to stand overnight. Precipitated asphaltenes were recovered by filtration (Whatman filter paper grade 42) and placed in a Soxhlet extractor equipped with *n*-heptane to extract co-precipitated maltenes. Cleaned asphaltenes were recovered by dissolution in toluene.

Extrography Fractionation Method. An extrography-based fractionation method was implemented as previously described.[2] In short, 250 mg of purified asphaltenes was dissolved in 400 mL of dichloromethane (DCM) in a round-bottom flask and mixed with 20 g of silica gel. The mixture was completely dried under a continuous stream of N_2. The adsorbed asphaltenes on silica gel were placed into a high-purity microglass thimble and Soxhlet-extracted with two solvent series. The first series consists of acetone and acetonitrile (ACN); the second series is a polarity gradient comprising *n*-heptane, 1:1 *n*-heptane/toluene, toluene, 1:1 Tol/THF, THF, and 4:1 THF/MeOH. The extraction period with each solvent lasted 24 h. Asphaltene fractions were dried under nitrogen.

Positive-Ion Atmospheric Pressure Photoionization [(+) APPI] FT-ICR MS Analysis. Asphaltenes, fractions, and maltenes were reconstituted in toluene to a final concentration of 200 μL/mL and infused into an APPI source at a flow rate of 50 μL /minute. A custom-built 9.4 T Fourier transform ion cyclotron resonance mass spectrometer was used for analysis as described previously.[31] Data collection was performed with Predator Acquisition Software, and spectra calibration and molecular assignments were performed by Predator Analysis[32,33] and PetroOrg software.[34]

Stored Waveform Inverse Fourier Transform (SWIFT) Excitation and Infrared Multiphoton Dissociation (IRMPD) of Asphaltenes. For structural analysis of asphaltenes, high-DBE (low mass defect)[35] compounds in a 4 Da range were isolated and fragmented by IRMPD. The technique is introduced in Figure 1 for a coal asphaltene fraction. A quadrupole isolation (top panel) is compared with the use of a multinotch SWIFT waveform[36] (in addition to quadrupole isolation, bottom). A quadrupole mass filter was used to isolate ions near m/z 460 (top panel); ions have mass defects from ∼0.0500 to 0.4000 Da, indicating a wide range of aromaticities, as elucidated by the isoabundance-contoured DBE versus carbon number plot for monoheteroatomic (N_1, O_1, S_1) precursor ions (circled in red). MS/MS of the quadrupole-isolated precursor ions was performed in the ICR cell (∼4.5×10^{-10} Torr) by IRMPD (λ = 10.6 μm, 40 W, 10−700 ms irradiation, Synrad CO_2 laser, Mukilteo, WA) to yield structural information about asphaltenes. Upon IRMPD, the fragmentation mass spectrum for the quadrupole isolation (top right) revealed high relative abundance

https://dx.doi.org/10.1021/acs.energyfuels.9b03527
Energy Fuels 2020, 34, 1492−1505

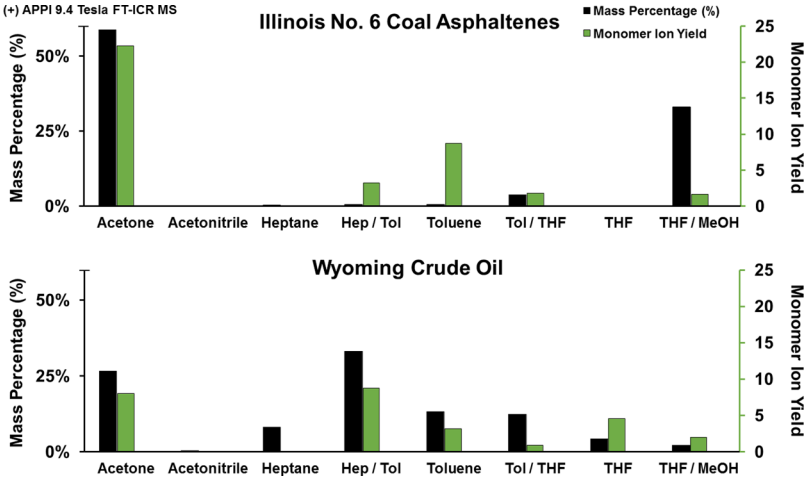

Figure 2. Mass distribution and monomer ion yield for asphaltene fractionation of (top) Illinois coal No. 6 whole C_7 asphaltenes and (bottom) Wyoming crude oil whole C_7 asphaltenes. These results illustrate differences in polarity and ionization efficiency between coal and petroleum fractions.

of low m/z ions (highlighted in yellow).[2] The DBE versus carbon number plot (precursor and fragments plotted together) indicates the presence of high- and low-DBE fragments. However, because ions with a wide range of DBE values were isolated as precursors, it is not possible to discern whether low-DBE fragments are produced from high-DBE multicore compounds or from low-DBE precursor ions.

Therefore, a SWIFT waveform (highlighted in green/blue) was applied to selectively isolate a 4 Da window at m/z 461−465 through ejection of ions outside of that window (high SWIFT amplitude). Furthermore, the SWIFT waveform was multinotch so that ions with a high mass defect (high hydrogen content/low DBE) are ejected from each nominal mass within the initial 4 Da isolation window. Thus, only ions between m/z 461−465 with a mass defect lower than 0.25000 Da remained in the ICR cell prior to fragmentation. The use of multiple notches increases the number of precursor ions and improves subsequent signal-to-noise ratio of IRMPD fragments. Small m/z ranges ensure similar molecular composition of precursor ions, which yield similar fragment ions. The isoabundance-contoured DBE versus carbon number plot for the SWIFT-isolated precursor ions (circled in red) illustrates the effectiveness of the multinotch SWIFT because only high-DBE ions are present prior to fragmentation. Upon IRMPD, the mass spectrum reveals both dealkylation (green) of the precursor ions, indicative of island motifs, and low m/z compounds. The zoomed inset (m/z 100−450) displays only the fragments (precursor excluded) because low m/z ions are not easily observed in the full mass spectrum (m/z 100−465) due to their low relative abundance. Thus, the approach is definitive in the identification of archipelago structural motifs even in the presence of low-DBE species within the same mass isolated window but suffers from reduced signal-to-noise in the IRMPD spectrum due to ion losses suffered in the multinotch SWIFT isolation of the high-DBE precursors (Figure 1, bottom right). Note that the low m/z fragments observed in the mass spectrum correlate with low-DBE/low carbon number fragment ions in the DBE versus carbon number plot and indicate losses of aromatic cores derived from multicore (high DBE) precursor ions. Therefore, the isolation/fragmentation method provides unambiguous evidence for the existence of archipelago motifs.

RESULTS AND DISCUSSION

Extrography Separation of Petroleum/Coal Asphaltenes and Ionization Efficiency. The gravimetric distribution of the extrography fractions can provide useful information for comparison of asphaltene samples because each fraction is enriched in different molecular motifs and presents different heteroatom contents. Therefore, the extrography separation helps to access such differences. The recovered mass of each extrography fraction is shown in black bars in Figure 2 and highlights the relative polarity of asphaltene compounds in each sample. Coal asphaltenes (Figure 2, upper panel) exhibit high relative abundance in acetone and THF/MeOH fractions, indicating the presence of more polar compounds than for Wyoming crude oil asphaltenes, which exhibit a more even mass distribution throughout all fractions.

The monomer ion yield (green bars) was calculated as previously described and is inversely proportional to the accumulation period required to collect a given number of ions for a sample at a given concentration.[1] Therefore, monomer ion yield reflects the production efficiency of non-aggregated asphaltene ions as measured by APPI coupled to FT-ICR MS. The latest/more polarizable extrography fractions (Tol/THF, THF, THF/MeOH) require a longer accumulation period to hit a target signal magnitude optimal for data collection, resulting in lower monomer ion yield. Previous work has suggested that the more polar/latest fractions contain asphaltenes that exhibit stronger aggregation trends than earlier extracted species (acetone and acetonitrile), which may be related to the presence of particular molecular motifs and active functionalities suitable for stronger intermolecular forces.[2] Petroleum asphaltenes display such behavior; for the second solvent series (from *n*-heptane to THF/MeOH), the monomer ion yield decreases as the solvent polarity increases, suggesting an inverse correlation between polarizability and ion production efficiency by APPI. Previous reports highlight stronger aggregation tendencies for Tol/THF and THF/MeOH subfractions extracted from geologically diverse asphaltenes.[2−4] The authors suggested a correlation between low ionization efficiency and asphaltene aggregation. Along those lines, we hypothesize that the low ionization efficiency of the THF/MeOH fractions from crude oil and coal asphaltenes may be related to stronger intermolecular forces. It is critical to point out the capability of THF/MeOH to disrupt hydrogen bonding, which we suggest is the dominant intermolecular force responsible for the retention of polar asphaltenes on silica gel. Therefore, the extraction of species with polar functional groups capable of hydrogen bonding with the silica gel is possible with THF/MeOH.

https://dx.doi.org/10.1021/acs.energyfuels.9b03527
Energy Fuels 2020, 34, 1492−1505

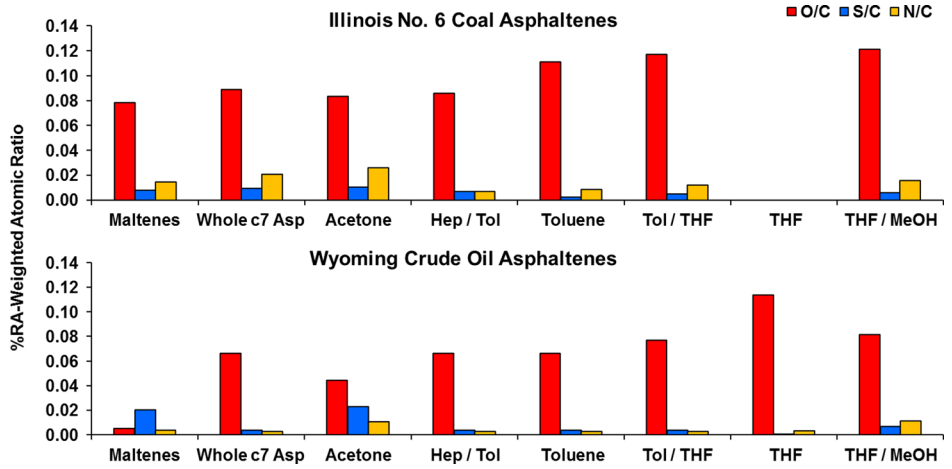

Figure 3. Progression of relative abundance-weighted atomic ratios (O/C, S/C, and N/C) for ions from the maltenes, whole C_7 asphaltenes, and extrography fractions derived from (top) Illinois coal No. 6 asphaltenes and (bottom) Wyoming crude oil asphaltenes. These results demonstrate that as solvent polarity increases, so does oxygen content (O/C ratio) for both coal and petroleum asphaltenes.

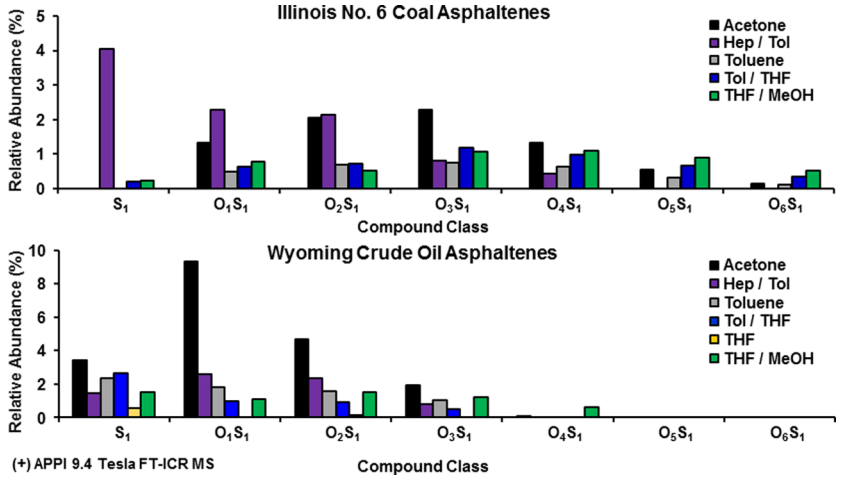

Figure 4. Relative abundances of S_1 and O_xS_1 ions for extrography fractions from (top) Illinois coal asphaltenes and (bottom) Wyoming crude oil asphaltenes. The Illinois coal No. 6 asphaltene fractions contain O_1S_1-O_6S_1 compounds, whereas the Wyoming crude oil asphaltene fractions contain O_1S_1-O_4S_1 species, in accord with the high oxygen content of Illinois coal asphaltenes.

Heteroatom Content. The heteroatom (O, N, S) content of asphaltenes can illuminate the behavior of a petroleum or coal sample because as heteroatom content increases, so do boiling point, aggregation tendency, and the tendency for water-in-oil emulsion stabilization.[37,38] Heteroatom content varies based on geographic origin, boiling cut, and between different fossil fuels (e.g., coal versus petroleum).[39,40] Typically, asphaltenes contain higher heteroatom content than their maltene counterparts because high heteroatom content increases the relative polarity of the oil and thus leads to increased precipitation in alkane solvents (such as C_7).[11] Crude oils with high heteroatom content typically exhibit a high tendency to aggregate, cause fouling problems, and form stable water-in-oil emulsions, and are therefore unfavorable for production and refinery purposes. Thus, knowledge of heteroatom content is critical to predict and overcome operational challenges for both coal- and petroleum-derived samples.

FT-ICR MS data was calibrated and peaks were assigned unique molecular formulas. Figure 3 presents the abundance-weighted atomic ratios (O/C, N/C, and S/C) for the maltenes, whole C_7 asphaltenes, and extrography fractions for coal and petroleum asphaltenes. Since each fraction is enriched in different heteroatom classes, we plot the atomic ratios so we can observe overall differences in oxygen, nitrogen, and sulfur content for each sample. Figure 3 demonstrates that as the solvent polarity increases for the second eluotropic series, the O/C ratio increases for both Illinois coal (top) and Wyoming crude oil (bottom) asphaltene samples. On the other hand, N/C and S/C ratios exhibit a bimodal distribution for both samples as the solvent polarity increases, with relative maxima for the acetone and THF/MeOH fractions. These results suggest that oxygen-containing functionalities play a central role in asphaltene adsorption onto SiO_2. Illinois coal asphaltenes exhibit higher relative abundance of oxygen-containing compounds than their petroleum counterparts, consistent with past coal asphaltene study findings.[5] The coal maltenes are also enriched in oxygen-containing species, in contrast to petroleum maltenes, which typically exhibit low heteroatom (in particular, oxygen) content relative to asphaltenes. As can be observed from Figure 2, coal asphaltenes had a low abundance in the THF fraction, and therefore we were unable to adequately characterize that fraction by FT-ICR MS.

https://dx.doi.org/10.1021/acs.energyfuels.9b03527
Energy Fuels 2020, 34, 1492−1505

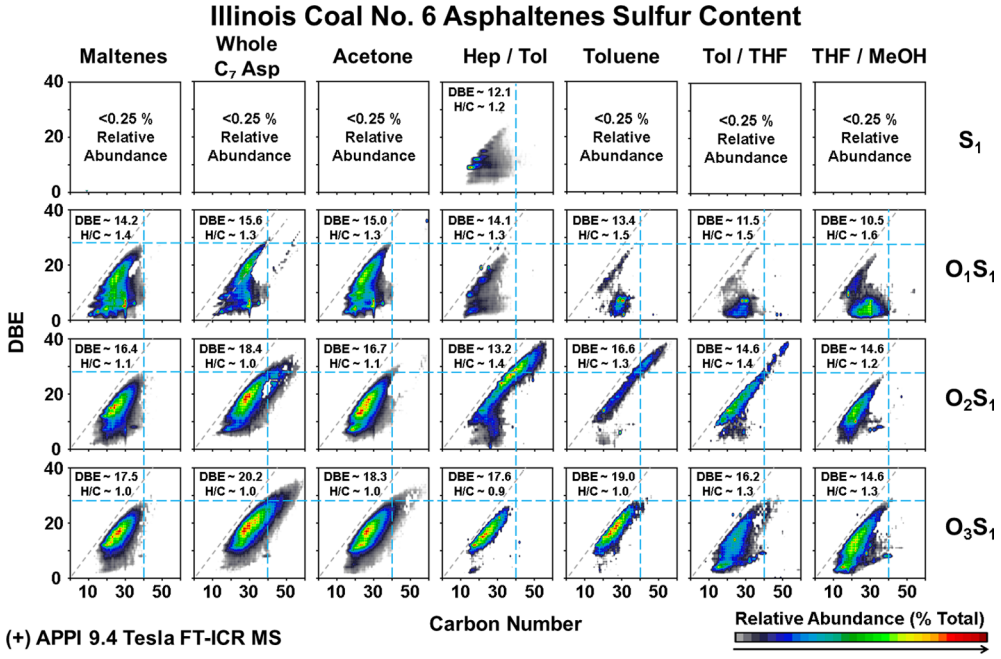

Figure 5. Isoabundance-contoured plots of DBE versus carbon number for S_1 and O_1S_1-O_3S_1 maltenes, whole C_7 asphaltenes, and their extrography fractions from Illinois coal No. 6 asphaltenes. These results demonstrate variability in the compositional range of O_xS_1 compounds among fractions of Illinois coal asphaltenes and reveal the presence of low-aromaticity asphaltenes in the later fractions.

Compositional Trends for S_1 and O_xS_1 Classes in Asphaltene Fractions. As illustrated by Figure 3, asphaltene fractions exhibit high oxygen content (O/C ratios) and notable amounts of sulfur. Therefore, we focus on the compositional trends for S_1 and O_xS_y species. Figure 4 shows the heteroatom compound class distributions for S_1 and O_xS_1 classes (O_1S_1-O_6S_1 for Illinois coal asphaltenes and O_1S_1-O_4S_1 for Wyoming crude oil asphaltenes) for the various fractions. As previously noted, the Illinois coal asphaltenes are enriched in oxygen-containing compounds; substantial amounts of higher-order oxygen-containing classes, O_5S_1-O_6S_1 species, are present in the most polarizable extrography fractions. The acetone, toluene, Tol/THF, and THF/MeOH fractions contain appreciable amounts of O_5S_1 and O_6S_1. The Hep/Tol fraction exhibits lower oxygen content and is enriched in nonpolar S_1 compounds, which are present in low abundance in the Tol/THF and THF/MeOH fractions. The compositional trends for the second solvent series suggest that the latest extrography fractions from coal asphaltenes are enriched in higher-order oxygen-containing classes. Several authors have suggested that the presence of multiple oxygen atoms per asphaltene molecule could promote stronger aggregation, adsorption on mineral surfaces, and emulsion stabilization tendencies.[16,41−44] Conversely, S_1 compounds are present in all fractions from Wyoming crude oil asphaltenes. From acetone to Tol/THF fractions, the relative abundances of the O_1S_1-O_3S_1 species exhibit a continuous decrease. The next fraction, THF, is depleted in S_1 species, and no appreciable amounts of O_1S_1, O_3S_1, or O_4S_1 are detected. The last and most polarizable fraction (THF/MeOH) exhibits higher relative abundances of O_1S_1-O_4S_1 than for Tol/THF, consistent with the elution of higher-order S_1O_x species in the coal asphaltenes.

Previous work has suggested that acetone and THF/MeOH enable the extraction of the most polar compounds as they are the strongest solvents used in both series.[2] However, intermolecular interactions between asphaltenes and the silica gel dictate which compounds are extracted in each fraction. Acetone has been demonstrated to predominantly extract highly aromatic, single-core (island) compounds that are capable of dipole−dipole interactions. The predominant intermolecular forces in acetone consist of dipole−dipole interactions. Conversely, THF/MeOH can extract compounds that are involved in hydrogen bonding with silica gel; because acetone is not able to participate in hydrogen bonding, hydrogen-bonding species remain on the silica gel until extraction with THF/MeOH. Although both solvents have high strength/polarity, they favor extraction of different species. For instance, the species extracted in the acetone fraction have been demonstrated to ionize efficiently (high monomer ion yield in Figure 2); such species exhibit weak aggregation upon *n*-heptane addition. On the other hand, the compounds extracted by THF/MeOH ionize poorly (lower monomer ion yield) and exhibit stronger aggregation.[2] Collectively, results regarding monomer ion yield heteroatom content and trends in class distribution suggest that hydrogen bonding correlates with low ionization efficiency.

Compositional Range for Coal Asphaltenes. Mass spectral data can then be displayed as isoabundance-contoured plots of DBE versus carbon number in which the color scale represents relative ion abundance. Therefore, as the compositional range progresses from low to high DBE values, compounds become more aromatic. For the same homologous series (i.e., constant DBE value and heteroatom class), the carbon number increases according to the number of additional $-CH_2$ groups. Figure 5 displays isoabundance-contoured plots of DBE versus carbon number for the S_1 and O_xS_1 heteroatom classes for coal maltenes and asphaltene extrography fractions.

Although the extrography fractions from Illinois coal reveal considerable similarities in their heteroatom content and compound class distribution, Figure 5 demonstrates that the compositional range for O_1S_1, O_2S_1, and O_3S_1 classes exhibits

https://dx.doi.org/10.1021/acs.energyfuels.9b03527
Energy Fuels 2020, 34, 1492−1505

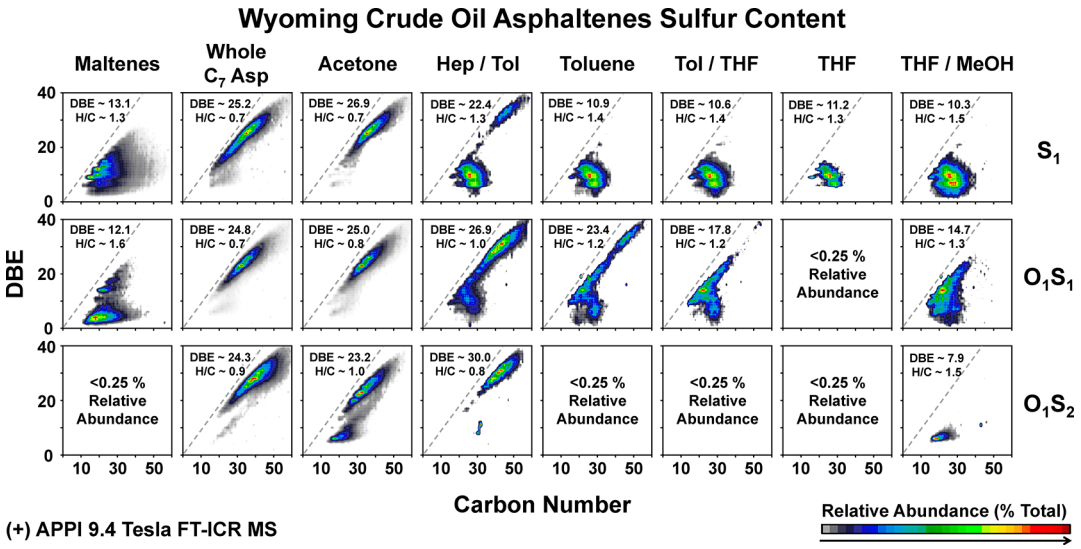

Figure 6. Isoabundance-contoured plots of DBE versus carbon number for S_1, O_1S_1, and O_1S_2 maltenes, whole C_7 asphaltenes, and their extrography fractions from Wyoming crude oil asphaltenes. Low-DBE O_xS_y compounds are observed for the later fractions of Wyoming crude oil asphaltenes and occupy a compositional range similar to that for Illinois coal asphaltenes.

significant differences from fraction to fraction. The first intriguing observation is that Illinois coal maltenes and whole C_7 asphaltenes span a similar compositional range. However, maltenes are slightly less aromatic than whole C_7 asphaltenes, as shown by their lower abundance-weighted DBE values and higher H/C ratios. The difference in compositional range is illustrated by blue lines at carbon number 40 and DBE 28; maltenes reside within that region, whereas the whole asphaltenes shift to higher carbon numbers and DBE values. With regard to the asphaltene extrography fractions, S_1 compounds are present at only >0.25% relative abundance for the Hep/Tol fraction, as shown by the heteroatom compound class distribution (Figure 4). The S_1 compounds for Hep/Tol occupy a compositional range close to the polycyclic aromatic hydrocarbon (PAH) limit, which represents the maximum DBE at a given carbon number for planar aromatics found in petroleum species.[45] Species with DBE values beyond the PAH limit include fullerenes, which have not been observed in petroleum. Note that the S_1 class, present only in the Hep/Tol fraction, displays high relative abundance of homologous series with DBE values at 9, 12, and 15. It is well known that alkylated dibenzothiophenes (three aromatic rings, DBE = 9), benzonaphthothiophenes (four aromatic rings, DBE = 12), and dinaphthothiophenes (five aromatic rings, DBE = 15) are stable sulfur-containing hydrocarbons that survive over geological time and thermal cracking processes in refineries.[16]

The compositional range for the acetone fraction closely resembles that for the whole C_7 asphaltenes, in agreement with its high monomer ion yield. As the number of oxygen atoms increases (O_1S_1 to O_2S_1 and O_2S_1 to O_3S_1), the compositional range shifts to higher aromaticity (higher abundance-weighted DBE and lower H/C ratio).

For the rest of the extrography fractions (Hep/Tol, Toluene, Tol/THF, and THF/MeOH), the compositional range for O_1S_1-O_3S_1 compounds generally shifts to lower aromaticity with increasing solvent polarity (rows, from left to right). An exception to that trend is that the toluene fraction exhibits slightly higher aromaticity than Hep/Tol for the O_2S_1 and O_3S_1 classes, in accord with the higher solvent aromaticity. It is worth noting that all compounds contain low-DBE O_1S_1 compounds (atypical for asphaltenes), especially the latest (most polarizable) fractions (toluene, Tol/THF, THF/MeOH), which are enriched in low-DBE atypical species (~15 to 40 carbon number, DBE < 10). Those low-DBE compounds occupy a compositional range similar to interfacial material extracted from asphaltenes from geologically diverse crude oils and bitumen samples.[38,46−48] Therefore, we hypothesize that these O_2S_1 and O_3S_1 species classify, in solubility terms, as asphaltenes because of their high heteroatom content and functionalities capable of hydrogen bonding. Hydrogen bonds between interfacially active petroleum compounds and water are well recognized as a cause for emulsion stability. We suspect that these low-DBE compounds, which occupy an atypical compositional range for asphaltenes, precipitate in *n*-heptane due to their functionality and/or structure rather than their aromaticity.[2]

Compositional Range for Petroleum Asphaltenes. Wyoming crude oil C_7 asphaltenes exhibit a compositional range closer to the polycyclic aromatic hydrocarbon (PAH) limit than their coal counterparts, as shown by the isoabundance-contoured DBE versus carbon number plots in Figure 6. Higher aromaticity in the Wyoming crude oil asphaltenes (relative to the coal asphaltenes) is observed by the higher DBE values and lower H/C ratios for the S_1 and O_1S_1 classes. The Wyoming crude oil maltenes present a compositional range with much lower DBE values than the whole C_7 asphaltenes, consistent with the typical molecular composition for petroleum maltenes.

The acetone fraction for Wyoming crude oil asphaltenes resembles the composition of the whole sample, a result consistent with its higher monomer ion yield than the rest of the extrography fractions. An exception to that trend is in the O_1S_2 class because the acetone fraction contains low-DBE species that are not present in high abundance in the whole C_7 asphaltenes.

Examination of the five fractions that comprise the polarity-gradient solvent series (Hep/Tol, toluene, Tol/THF, THF, THF/MeOH) reveals an atypical bimodal distribution for the compositional range (both high- and low-DBE values) for the

https://dx.doi.org/10.1021/acs.energyfuels.9b03527
Energy Fuels 2020, 34, 1492−1505

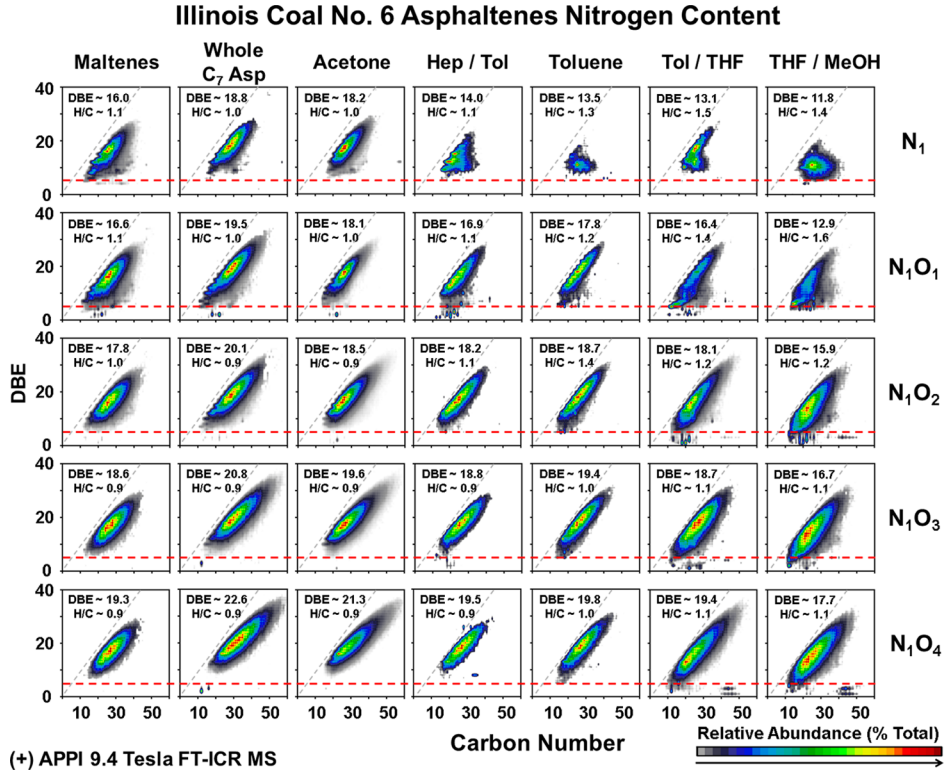

Figure 7. Isoabundance-contoured plots of DBE versus carbon number for N_1 and N_1O_1-N_1O_4 maltenes, whole C_7 asphaltenes, and their extrography fractions from Illinois coal No. 6 asphaltenes. The nitrogen-containing species for Illinois coal asphaltenes exhibit lower aromaticity as the solvent polarity increases (left to right).

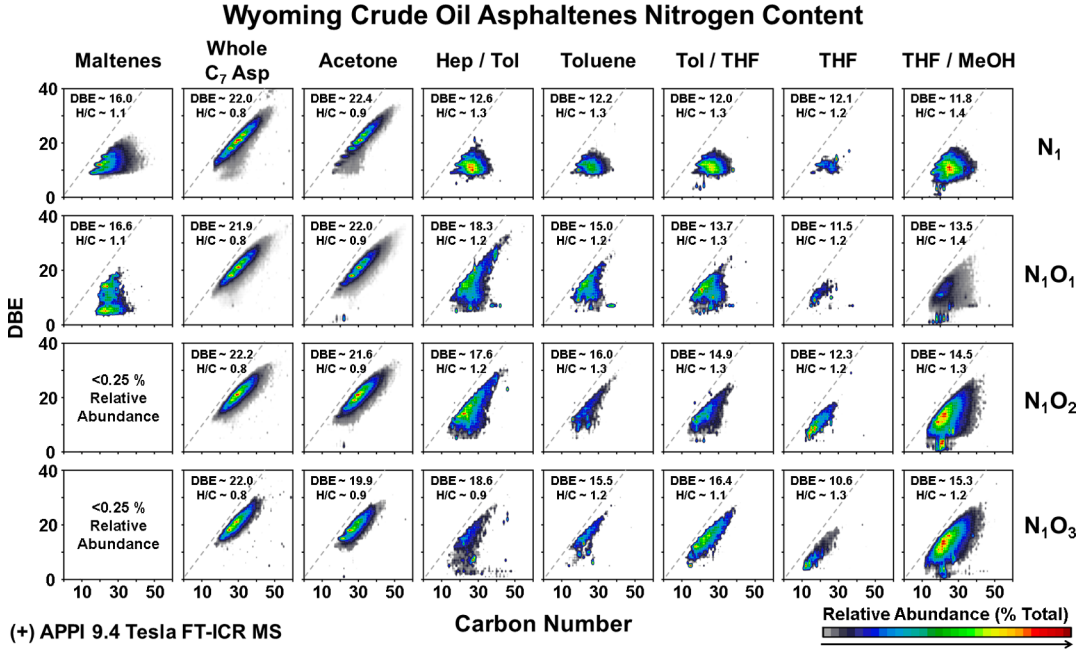

Figure 8. Isoabundance-contoured plots of DBE versus carbon number for N_1 and N_1O_1-N_1O_3 maltenes, whole C_7 asphaltenes, and their extrography fractions from Wyoming crude oil asphaltenes. The nitrogen-containing Wyoming crude oil asphaltenes also exhibit lower aromaticity as solvent polarity increases (left to right), as for Illinois coal asphaltenes.

S_1 and O_1S_1 classes. For the S_1 class in the Hep/Tol fraction, a classical asphaltene distribution close to the PAH limit is present, along with a low-DBE distribution. As the solvent polarity increases, the low-DBE distribution dominates the compositional range for the toluene, Tol/THF, THF, and THF/MeOH fractions. A similar trend is observed for the O_1S_1 class; however, the aromatic compounds remain along with the low-DBE species in the polar fractions. The presence of such atypical species is puzzling. We believe that low-DBE S_1 compounds likely correspond to remnant-occluded material.

https://dx.doi.org/10.1021/acs.energyfuels.9b03527
Energy Fuels 2020, 34, 1492−1505

A close examination of the S_1 compositional range reveals a high relative abundance for the homologous series with DBE values of 6, 7, 9, and 10 that likely correspond to alkylated benzo- and dibenzo-thiophenes with one cycloalkane ring, which are well recognized as petroleum biomarkers typically found in asphaltene-occluded compounds.[49,50]

For the O_1S_2 class, the most nonpolar fraction (Hep/Tol) contains high-DBE species that resemble the whole C_7 asphaltenes. For the Hep/Tol fraction, we hypothesize that S and O are embedded within the aromatic cores, in functionalities such as furan and thiophene, consistent with classical asphaltene chemistry. On the other hand, the most polar fraction (THF/MeOH) is enriched in low-carbon-number/low-DBE compounds that closely resemble the compositional range for interfacial material,[42,46,47] as pointed out for coal asphaltenes. An overall decrease in aromaticity is observed for all classes throughout the eluotropic solvent series (from the nonpolar Hep/Tol fraction to the polar THF/MeOH fraction), as demonstrated by lower DBE values and higher H/C ratios.

N_1 and N_1O_x Classes for Coal Compounds. Nitrogen-containing compounds are also present in coal maltenes, whole C_7 asphaltenes, and all asphaltene extrography fractions. Figure 7 shows isoabundance-contoured plots of DBE versus carbon number for N_1 and N_1O_x classes. As noted above, despite their different solubility behavior, the Illinois coal C_7 maltenes exhibit a molecular composition similar to C_7 asphaltenes and again exhibit lower abundance-weighted DBE values than whole C_7 asphaltenes.

For coal asphaltene species, as the solvent polarity increases, the compositional range for the extrography coal fractions progressively shifts to lower DBE values. The Tol/THF and THF/MeOH fractions include species with DBE values below 5 (line in red). Specifically, the N_1 class exhibits a shift to lower aromaticity in the most polar fractions, exemplified by lower DBE species than those in the acetone and Hep/Tol fractions. Although it is less dramatic than for the N_1 class, the N_1O_1-N_1O_4 classes also show lower aromaticity in the most polar fractions (Tol/THF and THF/MeOH) than in the nonpolar Hep/Tol and toluene fractions. The compositional trends seen in Figures 6 and 7 indicate that as more oxygen is incorporated (i.e., down a column for a specific fraction), the aromaticity increases for all fractions, suggesting that oxygen incorporation into coal species requires the presence of aromatic rings.

N-Containing Species for Petroleum Compounds. Although Wyoming crude oil asphaltenes exhibit lower nitrogen content than the Illinois Coal No. 6 (Figure 2), considerable amounts of N_1 and N_1O_1-N_1O_3 are present for the C_7 asphaltenes and extrography fractions. The compositional range for N-containing species for the Wyoming crude oil maltenes, C_7 asphaltenes, and extrography fractions is illustrated in DBE versus carbon number plots in Figure 8. Maltenes and whole C_7 asphaltenes occupy a complementary compositional range and petroleum maltenes exhibit lower oxygen content, lower carbon number, and lower DBE values than asphaltenes.[40] Therefore, maltenes are soluble in *n*-heptane. The Wyoming crude oil acetone fraction presents an almost identical compositional range to the whole C_7 asphaltenes, as seen for the O_xS_y species, in accord with its high monomer ion yield (4-fold higher than the Tol/THF fraction).

The rest of the extrography fractions, extracted with the polarity gradient solvent series (Hep/Tol to THF/MeOH), occupy compositional ranges that are considerably less aromatic than the whole C_7 asphaltenes and acetone fraction. For the N_1 class, the last five fractions (Hep/Tol, toluene, Tol/THF, THF, and THF/MeOH) are lower in aromaticity, with a compositional range that more closely resembles the maltenes than the whole asphaltenes. As discussed previously, that behavior is consistent with the composition of S_1 species for asphaltene extrography fractions from Wyoming crude oil and suggests that maltenic monoheteroatomic compounds found in asphaltenes may be remnant-occluded inside asphaltene networks. For polyheteroatomic species (N_1O_1, N_1O_2, N_1O_3), the aromaticity decreases as polarity increases, from Hep/Tol to THF. The latest fraction exhibits the lowest aromaticity; however, the aromaticity finally increases in the most polar (THF/MeOH) fraction. Furthermore, the THF/MeOH fraction, which has been shown to aggregate and ionize poorly by APPI compared to the rest of the extrography fractions, shows increased alkylation (longer homologous series) than the other fractions. The significantly lower aromaticity (lower abundance-weighted DBE and higher abundance H/C) for the latest extrography fractions (e.g., THF and THF/MeOH fractions, class N_1O_3) relative to the acetone fraction suggests that N_1O_x compounds in the latest fractions may exhibit functionalities capable of stronger intermolecular interactions such as hydrogen bonding. The low-DBE atypical species extracted with THF and THF/MeOH support such a hypothesis.

The results for N-containing species also demonstrate that aromaticity increases as a function of increasing oxygen content (Figure 8, proceeding down each column). Higher-order oxygen-containing classes (N_1O_2 and N_1O_3) exhibit higher abundance-weighted DBE values and lower H/C ratios. Exceptions to that trend are the toluene and THF fractions, N_1O_3 species, which exhibit low relative abundances for this compound class.

Fragmentation of Asphaltenes by IRMPD. Different trends in heteroatom compound content, aromaticity, and alkylation were observed from broadband mass spectra of the different extrography fractions. These results suggest that heteroatom content, aromaticity, and functionality may be responsible for the differences in asphaltene solubility and the behavior in mass spectrometry (monomer ion yield), as demonstrated previously.[2] Here, we seek to determine if there are trends in structural motifs that correlate with asphaltene behavior. We therefore employ IRMPD as a fragmentation method so that structural motifs and their relative abundances can be determined. Asphaltenes are isolated by external quadrupole isolation at m/z 462, followed by a multinotch SWIFT isolation, which, for each of several adjoining nominal mass ranges, selectively isolates the high-DBE precursor ions in the ICR cell and ejects the low-DBE precursors prior to fragmentation. In IRMPD, island/single-core compounds lose only the carbon number due to dealkylation but not aromaticity because the aromatic cores are stable. On the other hand, archipelago/multicore structures lose both the carbon number and DBE. Therefore, the selective isolation and subsequent fragmentation of high-DBE precursors for atypical samples that have both low- and high-DBE species (e.g., O_1S_1 species for the THF/MeOH fraction, Figure 5) enables determination of changes in DBE after dissociation and provides a basis to differentiate between island and archipelago motifs. This technique allows us to confidently conclude that any low-DBE fragments observed in the mass spectrum derive

https://dx.doi.org/10.1021/acs.energyfuels.9b03527
Energy Fuels 2020, 34, 1492−1505

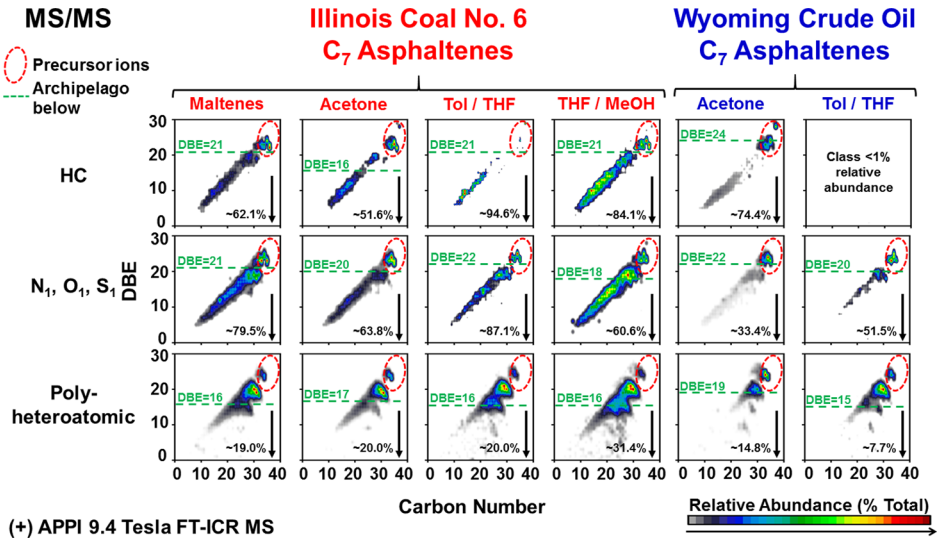

Figure 9. Isoabundance-contoured plots of DBE versus carbon number for hydrocarbon (HC), monoheteroatomic (S_1, O_1, N_1), and polyheteroatomic (e.g., O_2, N_2, O_1S_1, $O_1N_1S_1$, S_1O_3) classes for combined precursor and fragment ions for maltenes and fractions derived from coal and petroleum asphaltenes. The MS/MS results indicate that Illinois coal No. 6 is dominated by archipelago asphaltenes whereas the Wyoming crude oil asphaltenes are enriched in island-structure asphaltenes.

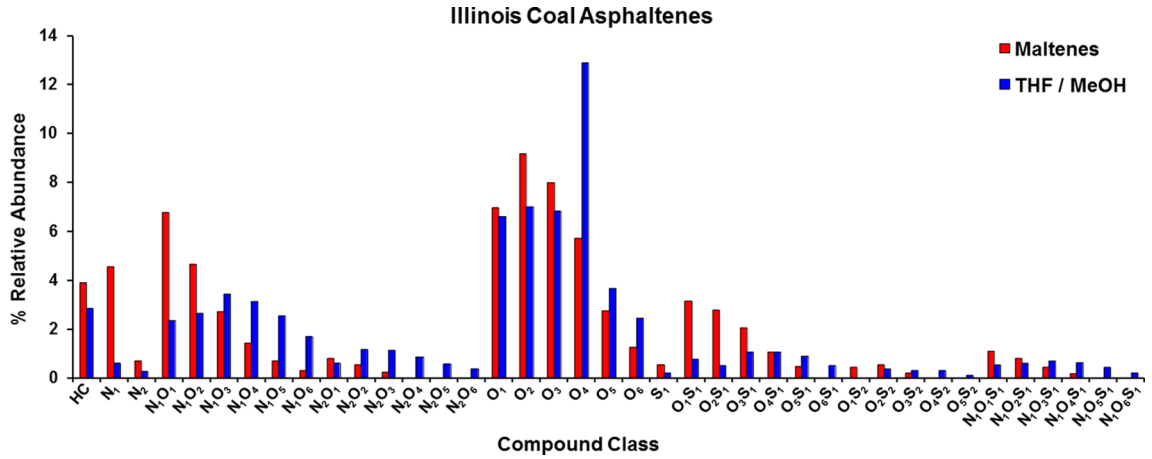

Figure 10. Heteroatom ion class distributions for Illinois coal No. 6 maltenes (red) and THF/MeOH asphaltene fraction (blue). Higher-order polyoxygenated species are observed for THF/MeOH but not for the maltenes, which may explain their differences in polarity despite similar O/C ratios (Figure 2).

from high-DBE precursor ions. As previously demonstrated by use of model compounds,[1] the infrared laser cleaves alkyl and cycloalkyl bridges between aromatic rings but does not break bonds within aromatic rings. Thus, island-type compounds produce no low-DBE fragments and exclusively show loss of carbon number (alkyl chains). Therefore, the presence of low-DBE fragments from high-DBE precursor ions indicates the presence of archipelago structure asphaltenes. Selected extrography fractions from coal and petroleum asphaltenes were subjected to MS/MS to determine the structural motifs in each sample.

Figure 9 displays the carbon number versus DBE plots for precursor ions (circled in red) and fragment ions. The island/archipelago boundary (dashed green line) is the lowest DBE value for a fragment to be considered island/single-core. Species with DBE values below that boundary are considered products from archipelago precursor ions. The island/archipelago boundary is calculated as the abundance-weighted average DBE value of the precursor ions minus its abundance-weighted standard deviation. The percentage of fragment ions below that boundary represents the relative fraction of fragmented species with an archipelago structure and has been shown to vary as a function of fraction, sample, and *m/z*.[2,3]

The more polarizable Illinois Coal No. 6 asphaltene fractions (Tol/THF, and THF/MeOH) exhibit high abundance of low-DBE fragments for the hydrocarbon (HC) and monoheteroatomic (N_1, O_1, and S_1) classes that indicate a contribution from archipelago-type compounds. For instance, the HC species for Illinois Coal No. 6 Tol/THF and THF/MeOH fractions exhibit ∼94 and ∼84% of the fragments with DBE values much lower than the island/archipelago boundary. Conversely, the acetone fraction contains more island-type compounds and exhibits lower percentage of fragments below the boundary line. The results agree with previous reports in which acetone was shown to preferentially extract large, highly aromatic single core asphaltenes, whereas Tol/THF and THF/MeOH contained a higher contribution of multicore

https://dx.doi.org/10.1021/acs.energyfuels.9b03527
Energy Fuels 2020, 34, 1492−1505

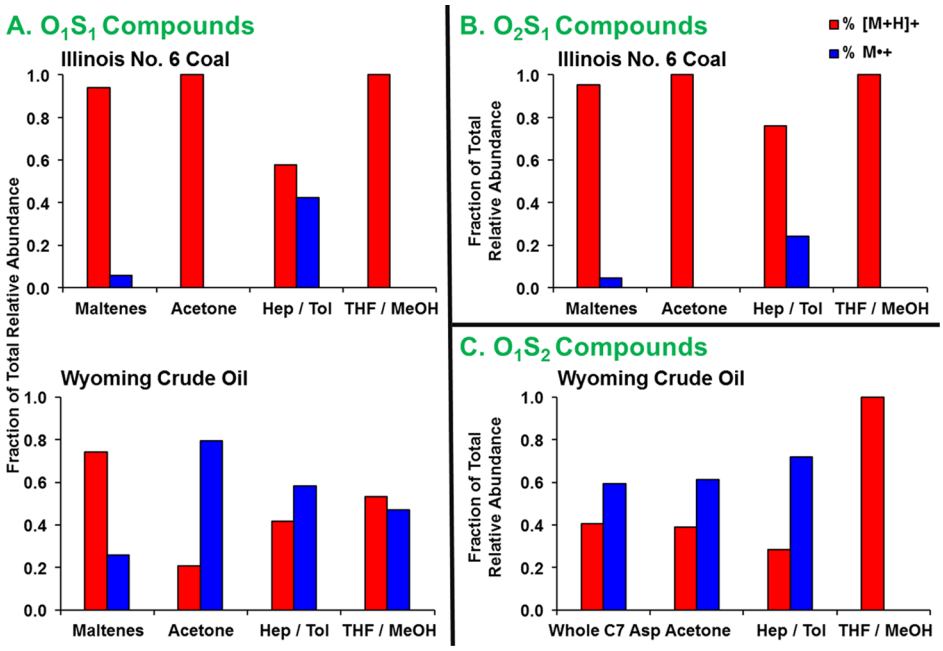

Figure 11. Relative abundance distributions of protonated ($[M + H]^+$, red) and radical ($M^{\cdot+}$, blue) cations for Illinois coal No. 6 and Wyoming crude oil maltenes and asphaltene extrography fractions. (A) O_1S_1, (B) O_2S_1, and (C) O_1S_2 are displayed. These results suggest that species that interact in hydrogen-bonding ionize as protonated cations rather than radical cations.

asphaltenes with higher oxygen content.[2,3] It is important to note that polyheteroatomic fragments were shown to be island-dominant across all coal maltene and asphaltene fractions, with a low percentage of fragments below the lower DBE limit. Such behavior is not evidence for the dominance of polyheteroatomic island structures. Detection of polyheteroatomic fragments (e.g., class N_1O_3) requires that all heteroatoms remain in the same aromatic core after IRMPD. However, archipelago/multicore structures in which heteroatoms are in separate aromatic cores will produce mono-heteroatomic fragments after IRMPD.

Surprisingly, Illinois Coal No. 6 maltenes displayed significant content of archipelago compounds for the HC and monoheteroatomic classes, with fragmentation patterns similar to those for the THF/MeOH fraction. This observation was unexpected because maltenes typically comprise easily ionizable compounds, a behavior strongly associated with island structures (See Figure S1 for the Wyoming crude oil maltenes (island-dominant)). Moreover, coal maltenes are also enriched in heteroatoms and exhibit a compositional range similar to that for the THF/MeOH fraction in some compound classes (Figures 3, 5, and 7). Therefore, the reason for the different solubility behavior for coal and asphaltenes maltenes despite their similar molecular composition is intriguing. Figure 10 may shed some light on this matter. Figure 10 provides the compound class distribution for coal maltenes and the THF/MeOH extrography fraction from coal asphaltenes.

Although the coal maltenes and THF/MeOH fraction exhibit similar abundance-weighted atomic ratios, their compound class distributions exhibit different trends. Specifically, the Illinois coal maltenes contain more lower-order oxygen-containing classes (N_1O_1, N_2O_1, O_2, O_1S_1, O_2S_2, $N_1O_1S_1$), whereas the THF/MeOH extract has more higher-order oxygen-containing compounds (polyoxygenated species, e.g., O_4, O_4S_1, $N_1O_3S_1$). For instance, maltenes show a decrease in relative abundance as the number of oxygen increases for a given class (e.g., from N_1O_1 to N_1O_2). In contrast, the THF/MeOH species exhibit a more Gaussian distribution for a given class group (i.e. N_1O_x, O_x, O_xS_1) as the number of oxygens increases. Moreover, the presence of higher-order oxygen-containing species in the coal THF/MeOH fraction relative to coal maltenes is illustrated by the high abundance of compounds with up to six oxygen atoms. We hypothesize that maltenes are depleted in polyoxygenated (polyfunctional) compounds; therefore, their intermolecular interactions are weaker than those in asphaltenic species in the THF/MeOH fraction. These intermolecular interactions can cause different compounds to have a cooperative effect and form aggregates.[51] Recent studies suggest that polyfunctional oxygenated species can participate in multiple intermolecular interactions, which have been previously discussed to strengthen asphaltene aggregation. Thus, heteroatom content and structure (island versus archipelago) alone cannot explain why some compounds precipitate in *n*-heptane (asphaltenes) while others dissolve (maltenes). Polyfunctionality appears to be a driving factor in asphaltene precipitation and aggregation because polyfunctional species can participate in more intermolecular interactions.

Wyoming crude oil asphaltenes do not exhibit significant losses of DBE after IRMPD. Wyoming species mostly undergo dealkylation (decrease of carbon number), which is consistent with the dominance of island structures. Although the Wyoming deposit sample was demonstrated to be island-dominant in a previous study,[3] the later fraction (Tol/THF) from Wyoming crude oil showed increased contributions from archipelago compounds for the mono-heteroatomic species. These results agree with prior observations that asphaltene samples, regardless their geological origin, source (coal or petroleum) and thermal maturity, are composed of a mixture of island and archipelago structures, and their relative contributions are sample-dependent.[1,3] The latest/polar

https://dx.doi.org/10.1021/acs.energyfuels.9b03527
Energy Fuels 2020, 34, 1492−1505

fractions (Tol/THF and THF/MeOH) are largely comprised of archipelago species, whereas early fractions (acetone and Hep/Tol) are enriched in island motifs.

Acetone, Hep/Tol, and THF/MeOH Radical Versus Protonated Cations. Coal and petroleum asphaltene fractions exhibit high abundances of O_xS_y species (Figure 4), and the more polarizable fractions occupy an atypical, low-aromaticity compositional range (Figures 4 and 5). The atypical compositional range for polarizable asphaltene species can be explained by their capability to hydrogen-bond. Therefore, those species have a solubility behavior consistent with asphaltenes because they can establish stronger intermolecular interactions. For (+) APPI, compounds may ionize as protonated ($[M + H]^+$) and/or radical ($M^{\cdot+}$) cations. Recent work suggests that petroleum-derived compounds that participate in hydrogen-bonding interactions ionize preferentially as protonated cations rather than radical cations.[53] Therefore, investigation of the relative abundances of radical versus protonated cations can help to explain differences in composition between fractions.

In Figure 11, we investigate the relative contributions from radical and protonated cations and display the fraction of the relative abundance from each type of cation (protonated or radical) relative to the combined relative abundance (sum of protonated and radical cations) for a given class. (A radical vs. protonated cation can be distinguished based on whether the DBE value for the ion is integer or half-integer.[52]) The relative contributions from radical and protonated cations for coal (top) and petroleum (bottom) asphaltene fractions for the O_1S_1 compound class (Figure 11A, left panel) suggests that O_1S_1 compounds in coal asphaltenes ionize more preferentially as protonated cations compared to crude oil asphaltenes. The Illinois coal O_1S_1 compounds in the acetone and THF/MeOH fractions ionize exclusively as protonated cations, whereas the Hep/Tol fraction (most nonpolar) O_1S_1 species appear to ionize as both radical and protonated cations. Conversely, the Wyoming crude oil acetone, Hep/Tol, and THF/MeOH fractions contain greater contributions from radical cations. The maltenes from both coal and petroleum ionize preferentially as protonated cations, with smaller contributions of radical cations.

The coal asphaltenes contain more O_2S_1 compounds, which ionize almost exclusively as protonated cations (Figure 11B, top panel) and show similar trends as the O_1S_1 class. The O_2S_1 species from the acetone and THF/MeOH (most polarizable) fractions ionize only as protonated cations, whereas the Hep/Tol fraction contains O_2S_1 species that also ionize as radical cations.

The O_1S_2 compounds from Wyoming crude oil occupy an atypical (low DBE) compositional range (Figure 6) for the THF/MeOH fraction, as illustrated by the atypical ionization trends in Figure 11C (bottom right panel). The whole C_7 asphaltenes, acetone, and Hep/Tol fractions ionize preferentially as radical cations, whereas 100% of the THF/MeOH O_1S_2 compounds ionize as protonated cations. Finally, the most polarizable (THF/MeOH) fractions from each sample ionize preferentially as protonated cations for all samples, in agreement with the hypothesis that these species participate in strong hydrogen-bonding interactions.

CONCLUSIONS

Illinois coal asphaltenes consist of oxygen-rich, polar compounds. The present extrography method enables observation of archipelago compounds in later-eluting fractions of coal and petroleum asphaltenes, revealing species not easily observed for the whole sample. Selective isolation of high-DBE compounds by multinotch SWIFT followed by fragmentation indicates the coexistence of island and archipelago motifs in both samples although coal asphaltenes contain a higher relative abundance of archipelago species than petroleum asphaltenes. The Illinois coal maltenes exhibit abundant heteroatoms relative to petroleum maltenes, with especially high oxygen content, but appear to be depleted in polyfunctional species relative to their asphaltene counterparts. Although both samples are oxygen-rich, Wyoming crude oil asphaltenes present more sulfur-containing classes, whereas Illinois coal asphaltenes have more nitrogen-containing species. Polyfunctional archipelago-type compounds, abundant in the most polarizable fractions of coal and petroleum asphaltenes, are demonstrated to ionize poorly, in agreement with previous reports that suggest that such species exhibit the strongest aggregation trends. The extrography method can be applied to coal and petroleum asphaltenes to demonstrate that all asphaltene samples are likely a mixture of island and archipelago structures. Archipelago compounds in both coal and petroleum can be accessed through separation methods and exhibit large differences in ionization efficiency. The determination of the existence of archipelago motifs in these samples (which contain a mixture of high and low DBE species) is possible only by the selective isolation of high DBE precursors by multinotch SWIFT, with subsequent fragmentation.

ASSOCIATED CONTENT

Supporting Information

The Supporting Information is available free of charge at https://pubs.acs.org/doi/10.1021/acs.energyfuels.9b03527.

Isoabundance-contoured plots of DBE versus carbon number for hydrocarbon (HC) species for precursor and fragment ions in the maltene fraction for Wyoming crude oil; table of mass yield from coal extraction by a Tol/THF/MeOH (9/9/2) solvent mixture; table of asphaltene yield from C_7 precipitation of a Tol/THF/MeOH coal extract; and table of asphaltene yield from C_7 precipitation of Wyoming crude oil (PDF)

AUTHOR INFORMATION

Corresponding Authors

Ryan P. Rodgers − *Department of Chemistry and Biochemistry, Ion Cyclotron Resonance Program, National High Magnetic Field Laboratory, and Future Fuels Institute, Florida State University, Tallahassee, Florida 32308, United States;* orcid.org/0000-0003-1302-2850; Phone: +1 850-644-2398; Email: rodgers@magnet.fsu.edu; Fax: +1 850-644-1366

Alan G. Marshall − *Department of Chemistry and Biochemistry and Ion Cyclotron Resonance Program, National High Magnetic Field Laboratory, Florida State University, Tallahassee, Florida 32308, United States*; Phone: +1 850-644-0529; Email: marshall@magnet.fsu.edu; Fax: +1 850-644-1366

https://dx.doi.org/10.1021/acs.energyfuels.9b03527
Energy Fuels 2020, 34, 1492−1505

Authors

Sydney F. Niles − *Department of Chemistry and Biochemistry, Florida State University, Tallahassee, Florida 32308, United States*

Martha L. Chacón-Patiño − *Ion Cyclotron Resonance Program, National High Magnetic Field Laboratory, Florida State University, Tallahassee, Florida 32310, United States;* orcid.org/0000-0002-7273-5343

Donald F. Smith − *Ion Cyclotron Resonance Program, National High Magnetic Field Laboratory, Florida State University, Tallahassee, Florida 32310, United States;* orcid.org/0000-0003-3331-0526

Complete contact information is available at: https://pubs.acs.org/10.1021/acs.energyfuels.9b03527

Notes

The authors declare no competing financial interest.

■ ACKNOWLEDGMENTS

Work was performed at the National High Magnetic Field Laboratory ICR User Facility, which is supported by the National Science Foundation Division of Chemistry through Cooperative Agreements DMR-1157490 and DMR-1644779, and the State of Florida.

■ REFERENCES

(1) Chacón-Patiño, M. L.; Rowland, S. M.; Rodgers, R. P. Advances in Asphaltene Petroleomics. Part 1: Asphaltenes Are Composed of Abundant Island and Archipelago Structural Motifs. *Energy Fuels* **2017**, *31*, 13509−13518.

(2) Chacón-Patiño, M. L.; Rowland, S. M.; Rodgers, R. P. Advances in Asphaltene Petroleomics. Part 2: Selective Separation Method That Reveals Fractions Enriched in Island and Archipelago Structural Motifs by Mass Spectrometry. *Energy Fuels* **2018**, *32*, 314−328.

(3) Chacón-Patiño, M. L.; Rowland, S. M.; Rodgers, R. P. Advances in Asphaltene Petroleomics. Part 3. Dominance of Island or Archipelago Structural Motif Is Sample Dependent. *Energy Fuels* **2018**, *32*, 9106−9120.

(4) Lin, Y.-J.; Cao, T.; Chacón-Patiño, M. L.; Rowland, S. M.; Rodgers, R. P.; Yen, A.; Biswal, S. L. Microfluidic Study of the Deposition Dynamics of Asphaltene Subfractions Enriched with Island and Archipelago Motifs. *Energy Fuels* **2019**, 1882.

(5) Yen, T. F. Structural Differences Between Asphaltenes Isolated from Petroleum and from Coal Liquid. *Chem. Asphaltenes* **1982**, 39−51.

(6) Hortal, A. R.; Hurtado, P.; Martínez-haya, B.; Mullins, O. C. Molecular-Weight Distributions of Coal and Petroleum Asphaltenes from Laser Desorption / Ionization Experiments. *Energy Fuels* **2007**, *21*, 2863−2868.

(7) Andrews, A. B.; Edwards, J. C.; Pomerantz, A. E.; Mullins, O. C.; Nordlund, D.; Norinaga, K. Comparison of Coal-Derived and Petroleum Asphaltenes by 13C Nuclear Magnetic Resonance, DEPT, and XRS. *Energy Fuels* **2011**, *25*, 3068−3076.

(8) Wang, W.; Taylor, C.; Hu, H.; Humphries, K. L.; Jaini, A.; Kitimet, M.; Scott, T.; Stewart, Z.; Ulep, K. J.; Houck, S.; et al. Nanoaggregates of Diverse Asphaltenes by Mass Spectrometry and Molecular Dynamics. *Energy Fuels* **2017**, *31*, 9140−9151.

(9) Hurt, M. R.; Borton, D. J.; Choi, H. J.; Kenttämaa, H. I. Comparison of the Structures of Molecules in Coal and Petroleum Asphaltenes by Using Mass Spectrometry. *Energy Fuels* **2013**, *27*, 3653−3658.

(10) Schuler, B.; Meyer, G.; Peña, D.; Mullins, O. C.; Gross, L. Unraveling the Molecular Structures of Asphaltenes by Atomic Force Microscopy. *J. Am. Chem. Soc.* **2015**, *137*, 9870−9876.

(11) Rathsack, P.; Kroll, M. M.; Otto, M. Analysis of High Molecular Compounds in Pyrolysis Liquids from a German Brown Coal by FT-ICR-MS. *Fuel* **2014**, *115*, 461−468.

(12) Fuchs, W.; Sandhoff, A. G. Theory of Coal Pyrolysis. *Ind. Eng. Chem.* **1942**, *34*, 567−571.

(13) Stihle, J.; Uzio, D.; Lorentz, C.; Charon, N.; Ponthus, J.; Geantet, C. Detailed Characterization of Coal-Derived Liquids from Direct Coal Liquefaction on Supported Catalysts. *Fuel* **2012**, *95*, 79−87.

(14) Mathews, J. P.; Chaffee, A. L. The Molecular Representations of Coal - A Review. *Fuel* **2012**, *96*, 1−14.

(15) Liu, F.-J.; Fan, M.; Wei, X.-Y.; Zong, Z. M. Application of Mass Spectrometry in the Characterization of Chemicals in Coal-derived Liquids. *Mass Spectrom. Rev.* **2017**, *36*, 543−579.

(16) Chacón-Patiño, M. L.; Blanco-Tirado, C.; Orrego-Ruiz, J. A.; Gómez-Escudero, A.; Combariza, M. Y. Tracing the Compositional Changes of Asphaltenes after Hydroconversion and Thermal Cracking Processes by High-Resolution Mass Spectrometry. *Energy Fuels* **2015**, *29*, 6330−6341.

(17) Schwager, I.; Farmanian, P. A.; Kwan, J. T.; Weinberg, V. A.; Yen, T. F. Characterization of the Microstructure and Macrostructure of Coal-Derived Asphaltenes by Nuclear Magnetic Resonance Spectrometry and X-Ray Diffraction. *Anal. Chem.* **1983**, *55*, 42−45.

(18) Wu, Z.; Jernström, S.; Hughey, C. A.; Rodgers, R. P.; Marshall, A. G. Resolution of 10 000 Compositionally Distinct Components in Polar Coal Extracts by Negative-Ion Electrospray Ionization Fourier Transform Ion Cyclotron Resonance Mass Spectrometry. *Energy Fuels* **2003**, *17*, 946−953.

(19) Castro-Marcano, F.; Mathews, J. P. Constitution of Illinois No. 6 Argonne Premium Coal: A Review. *Energy Fuels* **2011**, *25*, 845−853.

(20) Wu, Z.; Rodgers, R. P.; Marshall, A. G. Compositional Determination of Acidic Species in Illinois No. 6 Coal Extracts by Electrospray Ionization Fourier Transform Ion Cyclotron Resonance Mass Spectrometry. *Energy Fuels* **2004**, *18*, 1424−1428.

(21) Mckenna, A. M.; Purcell, J. M.; Rodgers, R. P.; Marshall, A. G. Identification of Vanadyl Porphyrins in a Heavy Crude Oil and Raw Asphaltene by Atmospheric Pressure Photoionization Fourier Transform Ion Cyclotron Resonance (FT-ICR) Mass Spectrometry. *Energy Fuels* **2009**, *23*, 2122−2128.

(22) Purcell, J. M.; Merdrignac, I.; Rodgers, R. P.; Marshall, A. G.; Gauthier, T.; Guibard, I. Stepwise Structural Characterization of Asphaltenes during Deep Hydroconversion Processes Determined by Atmospheric Pressure Photoionization (APPI) Fourier Transform Ion Cyclotron Resonance (FT-ICR) Mass Spectrometry. *Energy Fuels* **2010**, *24*, 2257−2265.

(23) Robb, D. B.; Covey, T. R.; Bruins, A. P. Atmospheric Pressure Photoionization: An Ionization Method for Liquid Chromatography-Mass Spectrometry. *Anal. Chem.* **2000**, *72*, 3653−3659.

(24) McKenna, A. M.; Marshall, A. G.; Rodgers, R. P. Heavy Petroleum Composition. 4. Asphaltene Compositional Space. *Energy Fuels* **2013**, *27*, 1257−1267.

(25) Vorres, K. S. The Argonne Premium Coal Sample Program. *Energy Fuels* **1990**, *4*, 420−426.

(26) Castro-Marcano, F.; Lobodin, V. V.; Rodgers, R. P.; McKenna, A. M.; Marshall, A. G.; Mathews, J. P. A Molecular Model for Illinois No. 6 Argonne Premium Coal: Moving toward Capturing the Continuum Structure. *Fuel* **2012**, *95*, 35−49.

(27) Larsen, J. W.; Wernett, P. Pore Structure of Illinois No.6 Coal. *Energy Fuels* **1988**, *2*, 719−720.

(28) Affolter, R. H.; Hatch, J. R. Characterization of the Quality of Coals from the Illinois Basin. In *Resource Assessment of the Springfield , Herrin , Danville , and Baker Coals in the Illinois Basin*; US Department of the Interior, 2002; pp E1−E230.

(29) Rodgers, R. P.; Mapolelo, M. M.; Robbins, W. K.; Chacón-Patiño, M. L.; Putman, J. C.; Niles, S. F.; Rowland, S. M.; Marshall, A. G. Combating Selective Ionization in the High Resolution Mass Spectral Characterization of Complex Mixtures. *Faraday Discuss.* **2019**, *218*, 29−51.

(30) Giraldo-Dávila, D.; Chacón-Patiño, M. L.; Orrego-Ruiz, J. A.; Blanco-Tirado, C.; Combariza, M. Y. Improving Compositional Space Accessibility in (+) APPI FT-ICR Mass Spectrometric Analysis of Crude Oils by Extrography and Column Chromatography Fractionation. *Fuel* **2016**, *185*, 45−58.
(31) Smith, D. F.; Podgorski, D. C.; Rodgers, R. P.; Blakney, G. T.; Hendrickson, C. L. 21 Tesla FT-ICR Mass Spectrometer for Ultrahigh-Resolution Analysis of Complex Organic Mixtures. *Anal. Chem.* **2018**, *90*, 2041−2047.
(32) Blakney, G. T.; Hendrickson, C. L.; Marshall, A. G. Predator Data Station : A Fast Data Acquisition System for Advanced FT-ICR MS Experiments. *Int. J. Mass Spectrom.* **2011**, *306*, 246−252.
(33) Xian, F.; Hendrickson, C. L.; Blakney, G. T.; Beu, S. C.; Marshall, A. G. Automated Broadband Phase Correction of Fourier Transform Ion Cyclotron Resonance Mass Spectra. *Anal. Chem.* **2010**, *82*, 8807−8812.
(34) Corilo, Y. E. *PetroOrg Software*; Omics LLC: Tallahassee, FL 2014.
(35) McKenna, A. M.; Chacón-Patiño, M. L.; Weisbrod, C. R.; Blakney, G. T.; Rodgers, R. P. Molecular-Level Characterization of Asphaltenes Isolated from Distillation Cuts. *Energy Fuels* **2019**, *33*, 2018−2029.
(36) Guan, S.; Marshall, A. G. Stored Waveform Inverse Fourier Transform (SWIFT) Ion Excitation in Trapped-Ion Mass Spectometry: Theory and Applications. *Int. J. Mass Spectrom. Ion Processes* **1996**, *157-158*, 5−37.
(37) Giraldo-Dávila, D.; Chacón-Patiño, M. L.; McKenna, A. M.; Blanco-Tirado, C.; Combariza, M. Y. Correlations between Molecular Composition and Adsorption, Aggregation, and Emulsifying Behaviors of PetroPhase 2017 Asphaltenes and Their Thin-Layer Chromatography Fractions. *Energy Fuels* **2018**, *32*, 2769−2780.
(38) Clingenpeel, A. C.; Rowland, S. M.; Corilo, Y. E.; Zito, P.; Rodgers, R. P. Fractionation of Interfacial Material Reveals a Continuum of Acidic Species That Contribute to Stable Emulsion Formation. *Energy Fuels* **2017**, *31*, 5933−5939.
(39) Calemma, V.; Iwanski, P.; Nali, M.; Scotti, R.; Montanari, L. Structural Characterization of Asphaltenes of Different Origins. *Energy Fuels* **1995**, *9*, 225−230.
(40) Chacón-Patiño, M. L.; Rowland, S. M.; Rodgers, R. P. The Compositional and Structural Continuum of Petroleum from Light Distillates to Asphaltenes: The Boduszynski Continuum Theory as Revealed by FT-ICR Mass Spectrometry. *In The Boduszynski Continuum: Contributions to the Understanding of the Molecular Composition of Petroleum* **2018**, 113−171.
(41) Chacón-Patiño, M. L.; Blanco-Tirado, C.; Orrego-Ruiz, J. A.; Gómez-Escudero, A.; Combariza, M. Y. High Resolution Mass Spectrometric View of Asphaltene−SiO_2 Interactions. *Energy Fuels* **2015**, *29*, 1323−1331.
(42) Kilpatrick, P. K. Water-in-Crude Oil Emulsion Stabilization: Review and Unanswered Questions. *Energy Fuels* **2012**, *26*, 4017−4026.
(43) Adams, J. J. Asphaltene Adsorption, a Literature Review. *Energy Fuels* **2014**, *28*, 2831−2856.
(44) Gray, M. R.; Tykwinski, R. R.; Stryker, J. M.; Tan, X. Supramolecular Assembly Model for Aggregation of Petroleum Asphaltenes. *Energy Fuels* **2011**, *25*, 3125−3134.
(45) Hsu, C. S.; Lobodin, V. V.; Rodgers, R. P.; McKenna, A. M.; Marshall, A. G. Compositional Boundaries for Fossil Hydrocarbons. *Energy Fuels* **2011**, *25*, 2174−2178.
(46) Clingenpeel, A. C.; Robbins, W. K.; Corilo, Y. E.; Rodgers, R. P. Effect of the Water Content on Silica Gel for the Isolation of Interfacial Material from Athabasca Bitumen. *Energy Fuels* **2015**, *29*, 7150−7155.
(47) Jarvis, J. M.; Robbins, W. K.; Corilo, Y. E.; Rodgers, R. P. Novel Method to Isolate Interfacial Material. *Energy Fuels* **2015**, *29*, 7058−7064.
(48) Stanford, L. A.; Rodgers, R. P.; Marshall, A. G.; Czarnecki, J.; Wu, X. A. Compositional Characterization of Bitumen / Water Emulsion Films by Negative- and Positive-Ion Electrospray Ionization and Field Desorption / Ionization Fourier Transform Ion Cyclotron Resonance Mass Spectrometry. *Energy Fuels* **2007**, *21*, 963−972.
(49) Chacón-Patiño, M. L.; Vesga-Martínez, S. J.; Blanco-Tirado, C.; Orrego-Ruiz, J. A.; Gómez-Escudero, A.; Combariza, M. Y. Exploring Occluded Compounds and Their Interactions with Asphaltene Networks Using High-Resolution Mass Spectrometry. *Energy Fuels* **2016**, *30*, 4550−4561.
(50) Frysinger, G. S.; Gaines, R. B. Separation and Identification of Petroleum Biomarkers by Comprehensive Two-Dimensional Gas Chromatography. *J. Sep. Sci.* **2001**, *24*, 87−96.
(51) Gawrys, K. L.; Spiecker, P. M.; Kilpatrick, P. K. The Role of Asphaltene Solubility and Chemical Composition on Asphaltene Aggregation. *Pet. Sci. Technol.* **2003**, *21*, 461−489.
(52) Purcell, J. M.; Rodgers, R. P.; Hendrickson, C. L.; Marshall, A. G. Speciation of Nitrogen Containing Aromatics by Atmospheric Pressure Photoionization or Electrospray Ionization Fourier Transform Ion Cyclotron Resonance Mass Spectrometry. *J. Am. Soc. Mass Spectrom.* **2007**, *18*, 1265−1273.
(53) Chacón-patiño, M. L.; Smith, D. F.; Hendrickson, C. L.; Marshall, A. G.; Rodgers, R. P. Advances in Asphaltene Petroleomics. Part 4. Compositional Trends of Solubility Subfractions Reveal That Polyfunctional Oxygen-Containing Compounds Drive Asphaltene Chemistry. Submitted for publication to *Energy Fuels*, December **2019**.

https://dx.doi.org/10.1021/acs.energyfuels.9b03527
Energy Fuels 2020, 34, 1492−1505